



**Article type: A-Regular research paper**

# Microstructure of zirconium carbide ceramics synthesized by spark plasma sintering

**B.A.B. Alawad\* (1)(2), H.A.A. Abdelbagi (2)(3), T.P. Ntsoane (4), T.T. Hlatshwayo (2)**

(1) *Department of Physics, Sudan University of Science and Technology, Sudan, alawad20024@gmail.com.*

(2) *Department of Physics, University of Pretoria, South Africa, Heshamabdelbagi100@gmail.com.*

(3) *Physics Department, Shendi University, Sudan, Heshamabdelbagi100@gmail.com.*

(4) *Radiation Science Division, South Africa Nuclear Energy Corporation (Necsa), South Africa, tshepo.ntsoane@necsa.co.za.*

**\*Corresponding author: [alawad20024@gmail.com](mailto:alawad20024@gmail.com)**

RECEIVED: 05 March 2022 / RECEIVED IN FINAL FORM: 15 April 2022 / ACCEPTED: 23 April 2022

**Abstract :** Zirconium carbide (ZrC) samples were prepared by spark plasma sintering (SPS), at temperatures of 1700 °C, 1900 °C and 2100 °C, all at pressure of 50 megapascal (MPa). The density of ZrC ceramic pellets was measured using a Micromeritics AccuPyc II 1340 Helium Pycnometer. The density of ZrC ceramic pellets was found to increase from  $(6.51 \pm 0.032)$  g/cm<sup>3</sup> to  $(6.66 \pm 0.039)$  g/cm<sup>3</sup> and  $(6.70 \pm 0.017)$  g/cm<sup>3</sup> when the temperature of the SPS was increased from 1700 °C to 1900 °C and 2100 °C respectively. Moreover, the hardness of ZrC ceramic pellets were measured using Rockwell hardness test. The hardness of ZrC ceramic pellets increased from  $(7.4 \pm 0.83)$  to  $(17.0 \pm 0.073)$  and  $(18.4 \pm 0.05)$  gigapascals (GPa) at temperatures of 1700 °C, 1900 °C and 2100 °C respectively. X-ray diffraction shows the absence of spurious phases or impurity. XRD results showed that, all prepared ZrC samples has the same preferred orientation of the planes (i.e., 200). Furthermore, the average grain size of ZrC was calculated using Sherrers's equation. The average grain size of the pure ZrC powder increased from 67.46 nm to 72 nm, 79 nm and 83 nm when the ZrC powder was sintered at temperatures of 1700 °C, 1900 °C and 2100 °C respectively. The differences in the average grain size between the prepared samples leads to show different surface morphologies that monitored by scanning electron microscopy (SEM).

**Keywords :** Zirconium carbide; Ceramic pellets; Zirconium carbide powder; Spark plasma sintering, sintering temperature.

**Cite this article:** B.A.B. Alawad, H.A.A. Abdelbagi, P.N. Ntsoane, T.T. Hlatshwayo, *OAJ Materials and Devices*, Vol. 6 (1), p0408-1 (2022) - DOI: 10.23647/ca.md20220408

## Introduction

ZrC is refractory ceramic material, it has attracted considerable attention due to its high melting point (3541 °C), low density (6.73 g/cm<sup>3</sup>), high hardness (25.5 GPa), high electrical conductivity (78 × 10<sup>-6</sup> Ω cm), high modulus of elasticity (350 - 440 MPa), good thermal shock resistance and solid-state phase stability [1-3]. Due to its excellent properties, ZrC material is a promising candidate for many applications such as coating of nuclear particles fuels and ultra-high temperature applications [4, 5]. ZrC ceramic pellets can be prepared by the chemical vapor deposition or spark plasma sintering. SPS is a sintering technique utilizing uniaxial force and a pulsed direct electrical current under low atmospheric pressure to perform high speed consolidation of the powder [6]. It provides rapid densification for different types of materials such as ZrC and hafnium carbide (HfC) [7]. This direct way of heating allows the application of very high heating and cooling rates, enhancing densification over grain growth promoting diffusion mechanisms allowing maintaining of the intrinsic properties of nano-powders in their fully dense products [8-10]. SPS systems offer many advantages over conventional systems using hot press sintering, hot isostatic pressing or atmospheric furnaces. Including ease of operation and accurate control of sintering energy as well as high sintering speed, high reproducibility, safety and reliability [8, 11]. While similar in some aspects to hot press, the SPS process is characterized by the application of the electric current through a power supply, leading to very rapid and efficient heating [8]. In SPS, densifications and sinter ability of ZrC can improved by metallic additive such as Ni, Mo, and their alloy [12, 13]. However, this can degrade the high temperature properties and corrosion resistance of ZrC [12-14]. For this reason, no additives were added in the ZrC samples sintered. Spark plasma sintering technique is a promising approach to improve the densification of ZrC at high temperature [6]. Previous study reported that, pressure assisted sintering at high sintering temperature to obtained dense ZrC ceramic [7]. In this work, the ZrC powder was compressed using SPS at pressure of 50 MPa and at different temperatures (i.e., 1700 °C, 1900 °C and 2100 °C). In this paper, the effect of sintering temperature on the

microstructures, density, and hardness of the obtained ZrC ceramics was investigated.

## Experimental procedure

Copy The raw materials used were zirconium carbide powder (mean particle size of 67.46 nm and purity >99 %) from Sigma-Aldrich. The ZrC powder was weighed using an electronic mass balance, so that equal amounts of the ZrC powder were used for the spark plasma sintering (SPS) process. The powders were prepared in a 20 mm inner diameter graphite die. Graphite foil with a thickness of 0.2 mm was placed between the die and powder for easy removal and to ensure that the cooling of the sintered ZrC samples was homogeneous. The outside of the graphite die was covered with an insulating felt to reduce radiation loss [15]. After the powder was placed in the graphite die, it was first cold pressed using a hydraulic press to consolidate the powder together and then spark plasma sintered (SPS). The ZrC ceramic pellets were sintered by SPS using the HHPD-25 from FCT System GmbH Germany at Tshwane University of Technology (see Fig. 1) [16]. The SPS process was conducted at temperatures of 1700 °C, 1900 °C and 2100 °C at a heating rate of 100 °C/min in vacuum (0.05 bar) until the desired temperature was attained. The holding time and pressure for sintering were 10 minutes and 50 MPa respectively. At the end of the sintering cycle, the specimens were rapidly cooled to room temperature. The samples of 20 mm diameter and approximately 5 mm thickness were attained. The samples were then cut into smaller pieces by a diamond saw, thereafter, polished using a Saphir 550 Semi-Automatic Grinder/Polisher. The samples were then cleaned in an ultrasonic bath using demineralized water and then ethanol for 5 min each. Then, the samples were dried in an oven at 100 °C for 30 min. Fig. 2 shows variation in pressure, displacement and temperature versus time regime during the sintering process at 1700 °C, 1900 °C and 2100 °C – see Fig. 2 (a), (b) and (c) respectively. At the end of the sintering cycle, the specimens were rapidly cooled to room temperature. The bulk densities of the as-sintered ZrC samples were measured by Archimedes' technique (using a Micromeritics Accupyc II 1340 fully automated pycnometer at University of Pretoria), this was done after removing the outer layer by polishing. The Vickers hardness was measured on a hardness tester (Rockwell Hardness testing machine at University of Pretoria) with an indentation load of 10 kg and a dwell time of 10 s.

The phase composition of the sintered ZrC samples was analyzed by X-ray diffraction (using Bruker XRD D8 Advance) with a CuK<sub>α</sub> radiation source ( $\lambda = 1.54056 \text{ \AA}$ ) within the recording range of 15 to 125° and a step size of 0.04°. The grain sizes of samples were measured from the XRD patterns using Sherrers's equation as given by equation (1) below [17]. Furthermore, the preferred orientation of the planes of the sintered ZrC samples was determined from the texture coefficient of the planes as given by equation (2) [18].

$$D = \frac{K\lambda}{\beta \cos\theta} \tag{1}$$

where  $D$  is the average grain size,  $\beta$  is the full width at half maximum (FWHM) of the diffraction peak,  $\theta$  is the Bragg angle (i.e., position of the peak),  $K$  is a constant (a value of 0.94 was used),  $\lambda$  is the wavelength of the excitation X-rays which is equals 1.54056 Å for CuK $\alpha$  radiation source.

$$TC = \frac{I(hkl)/I_o(hkl)}{N^{-1} \sum I(hkl)/I_o(hkl)} \tag{2}$$

where  $TC(hkl)$  is the texture coefficient of the  $hkl$  plane,  $I(hkl)$  is the measured relative intensity of a plane taken from the raw data of XRD,  $I_o(hkl)$  is the standard intensity of the plane taken from the International Centre for Diffraction Data (ICDD) database,  $N$  is the number of planes considered. The morphology of the ZrC surface layer were observed by scanning electron microscopy (SEM) (Zeiss Ultra Plus) with operating voltage of 1 kV.

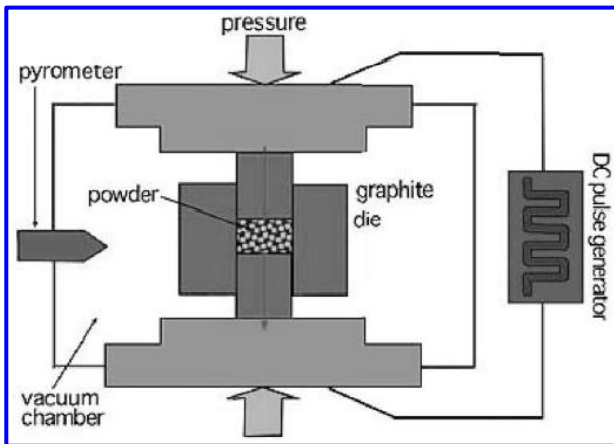


**Fig. 1. Schematic diagram of spark-plasma sintering (SPS).**

## Results and discussion

### 1. Density and Vickers hardness measurements

The relative density of ZrC increased with the sintering temperature from 96.6 % at 1700 °C and reached a maximum of 99.5 % at 2100 °C. The relative density of the ZrC ceramics from Sciti *et al.* [19] after sintering at 2100 °C was about 99 %. They used ZrC powders with mean particle size of 3.8 μm and their sample was sintered for only 3 min but at a higher

pressure of 65 MPa. Sun *et al.* [20] performed reactive spark plasma sintering (RSPS) using zirconium oxide (ZrO<sub>2</sub>) and carbon black to obtain ZrC whose relative density increased with the sintering temperature and reached 96.1% at 1900 °C. Therefore, as seen from the results in Table 1 and the results from other studies [19,20], it can be observed that higher densification of ZrC carbide is obtained as the sintering temperature increased. The relative density increases with temperature from 1700 to 2100 °C, and the grains coalesce to form denser clusters. The density did not reach the theoretical density of ZrC which is about 6.73 g/cm<sup>3</sup>, due presence of minute amounts of free carbon. Sun *et al.* [20] and Sciti *et al.* [19] obtained Vickers hardness values of 16.3 and 17.9 GPa from ZrC sintered at 1900 °C and 2100 °C respectively. The hardness values obtained in this study were 17.0 and 18.4 GPa after sintering ZrC at 1900 °C and 2100 °C respectively. These hardness values are slightly higher compared to those obtained by Sun *et al.* and Sciti *et al.* This is due to the longer sintering duration of 10 min at a lower pressure of 50 MPa at 2100 °C compared to 3 min and 65 MPa used by Sciti *et al.* [19]. It can be observed that longer sintering durations can lead to lower porosity therefore high density and high hardness values. The number of pores of the ZrC sintered at different temperatures were observed by scanning electron microscopy (SEM) and the results are discussed in section 3.3.

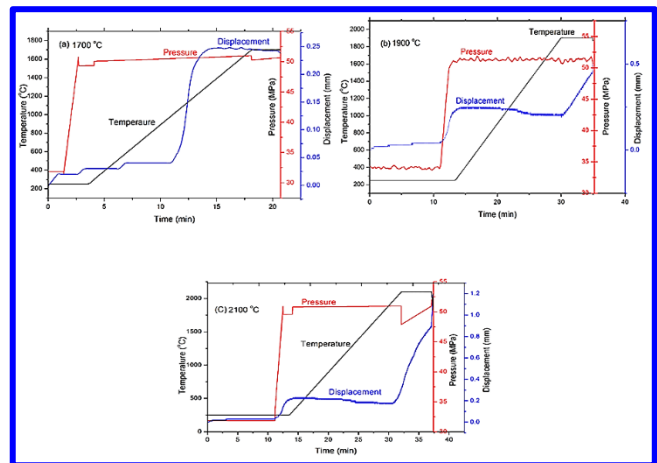


**Fig. 2. The graphs of pressure, displacement and temperature versus time regime during the sintering process at (a) 1700 °C (b)1900 °C (c) 2100 °C.**

### 2. XRD analysis

The phase composition of the bulk as-sintered ZrC samples was analysed by X-ray diffraction analysis (with an X-ray exposure time of 2 seconds for each step). The XRD patterns of ZrC samples sintered at 1700 °C, 1900 °C and 2100 °C are shown in Fig. 3. The diffraction peaks indicate the polycrystalline structure of the SPS synthesised ZrC. The all samples had similar peaks, and their intensities were observed to vary slightly. The XRD patterns of the prepared ZrC samples by SPS showed that all peaks are belong to the ZrC crystalline peaks. There did not appear to be any extra peaks, indicating there were no impurities present. Since the starting materials were pure ZrC powders, the XRD results was expected.

**Table 1: Relative density and hardness of ZrC prepared by SPS at 1700 °C, 1900 °C and 2100 °C and compared with the data from previous studies [19, 20].**

Material	Sintering conditions (°C/min/MPa)	Mean grain size (µm)	Relative Density (%)	Vickers hardness (GPa)	Reference
ZrC	1700/10/50	0.072	96.5	7.4 ± 0.83	This study
ZrC	1900/10/50	0.079	98.9	17.0 ± 0.073	This study
ZrC	2100/10/50	0.083	99.5	18.4 ± 0.05	This study
ZrC	1850/10/60	Around 2	85.3	9.1 ± 1.40	[20]
ZrC	1900/10/60	<10	96.1	16.3 ± 1.60	[20]
ZrC	2100/3/65	13 ± 1	99.0	17.9 ± 0.60	[19]

The ZrC peaks became slightly sharper at 2100 °C but the peak intensities were slightly lower than those obtained at 1700 °C and 1900 °C. The change in the peak intensity might be due to the change in the ZrC grain size, which will be discussed in more details in the next paragraph. The preferred orientation determined from the texture coefficient of the planes (given by equation (2) above) of the ZrC prepared by SPS at 1700 °C, 1900 °C and 2100 °C was found to be (200). The grain sizes of the ZrC samples were calculated using Sherrers’s equation (i.e., equation (1)). The calculated grain size of the pure ZrC powder (manufactured by Sigma-Aldrich with 99.9% purity) was found to be 67.46 nm. The average grain size was observed to increase from 71.88 ± 3.6 to 83.59 ± 3.9 nm after sintering from 1700 °C to 2100 °C, at 50 MPa for 10 min, respectively. Increasing the sintering temperature will increase the mobility of ZrC atoms led to the increase in average grain size, in line with crystal growth theory [21,22]. In comparison to previous studies by Sciti *et al.* [19, 23] who investigated the sinter ability of commercial ZrC powders with mean particle size of 3.8 µm (they did not report the grain or crystallite size), however, they measured the grain size for the obtained dense ZrC ceramics. They found that the grain size increased from 5.8 ± 1 to 13 ± 1 µm after sintering at temperatures from 1900 to 2100 °C, pressure of 65 MPa and time of 3 min. This indicated that the starting materials, sintering conditions and the application of very high heating and cooling rates led to form larger grain sizes at higher temperatures which enhanced higher densification. Sciti *et al.* [23], measured the grain sizes of their SPS prepared ZrC samples through image analysis on SEM micrographs using the Image Pro Plus Software. However, in this study, the crystallite size was calculated from XRD spectra using

Sherrers’s equation (i.e., equation (1)). Therefore, these are fundamentally different results and not comparable with our results, since a particle often has more than one grain. The overall trend is an increase in grain size of ZrC with increasing temperature. It is well known that the average grain size of a film increases with increasing temperature as reported by Thompson *et al.* [24]. This is due to the increasing mobility of the atoms at higher temperature.

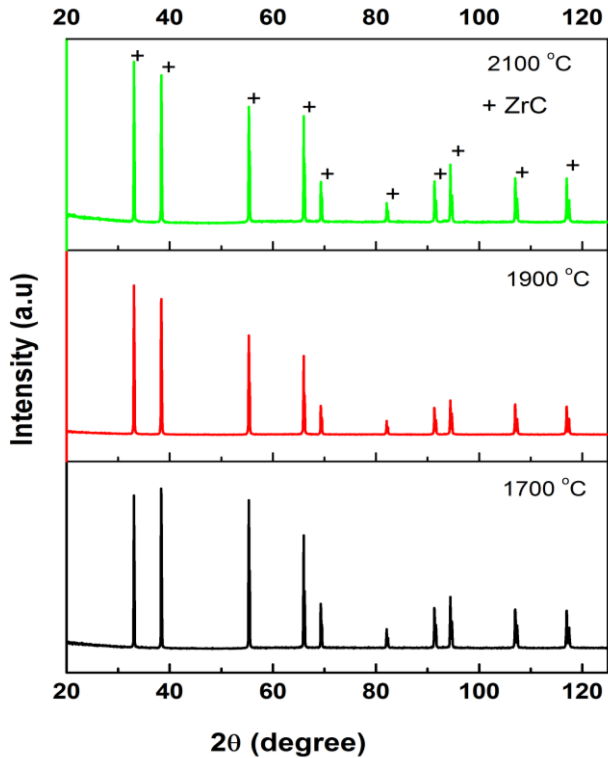


**Fig. 3. XRD patterns of ZrC ceramics produced by SPS in 1700 °C, 1900 °C and 2100 °C.**

### 3. SEM analysis

The SEM images (obtained by secondary electron mode) from the surface of the ZrC samples sintered to different final temperatures allowed the investigation of the microstructure evolution during the SPS. However, the contrast in these images is not appropriate to make grain size comparison easy. This could be due to the large pores that can trap the secondary electrons generated. The surface of ZrC sintered at 1700 °C is given in Fig. 4 (a) and the surface can be observed to be inhomogeneous and coarse. This is due to agglomeration and coalescing of the fine ZrC particles to form larger ones during sintering. This led to a highly porous structure at this sintering temperature. The presence of these pores in the surface of ZrC samples sintered at 1700 °C can explain the lower relative density of the sample

obtained (96.5 %) – see Table 1. Furthermore, the structural changes due to sintering at different temperatures can be deduced from the SEM micrographs as seen in Fig. 4 (a), (b) and (c). The surface of ZrC sample sintered at 1900 °C (Fig. 4 (b)) is still inhomogeneous, it is denser with a lower number of pores compared to the sample sintered at 1700 °C. The inhomogeneous surface consists of particles of different sizes. The reduced pore size and density accounts for the increase in relative density of this sample to 98.9% and increase in particle size after sintering at 1900 °C – see Fig 4 (b) and Table. 1. As mentioned above, increasing the sintering temperature can decrease the number of pores due to growth of the crystallites at higher temperatures. The surface of the sample sintered at 2100 °C has fewer and smaller pores (with relative density of 99.5 %) compared to the sample prepared at 1900 °C which had larger and more pores. The surface looks smoother compared to the 1700 °C and 1900 °C prepared samples and the grains are lying flat on a surface. The SEM micrographs of ZrC sintered at 1700 and 2100 °C illustrate how the ZrC surface morphology changed with the relative density. These changes led to an increase in relative density and hardness from 96.5% and 7.4 GPa at 1700 to 99.5% and 18.4 GPa at 2100 °C, respectively. In Fig. 4(c), more consolidated surface structure appears in the specimens. Therefore, from Fig. 4 and Table 1, the sintering temperature determines the level of densification of ZrC as well as the crystallite size growth. The progress of enhanced densification and crystallization phenomena with increase in the sintering temperature might be due to accelerated surface diffusion and grain boundary diffusion at the higher temperatures [25].

## Conclusion

ZrC was synthesised by SPS at various temperatures. The phase and microstructure evolution after the ZrC sintering process at 1700 °C, 1900 °C and 2100 °C was investigated by SEM. The relative density of ZrC prepared by SPS was seen to increase as sintering temperature increased. This is due to the increase in the grain size of ZrC as the sintering temperature increased. The growth of the grain will lead to the closure of the pores. Thus, the reduction in the pore size will led to the increase in relative density high temperatures sintered samples. Moreover, the reduction in the pore number and size causes the hardness of ZrC to be increased. The preferred orientation of the ZrC sintered at 1700 °C to 2100 °C was found to be the (200) plane. The surface of the as-sintered samples was observed to vary with sintering temperatures. The ZrC surface was generally uneven, heterogeneous and had agglomerated granules with the number and size of pores decreasing with increasing the sintering temperature.

## Acknowledgements:

Financial support by the National Research Foundation of South Africa (grant numbers 120808, 120471 and 120804) is gratefully acknowledged.

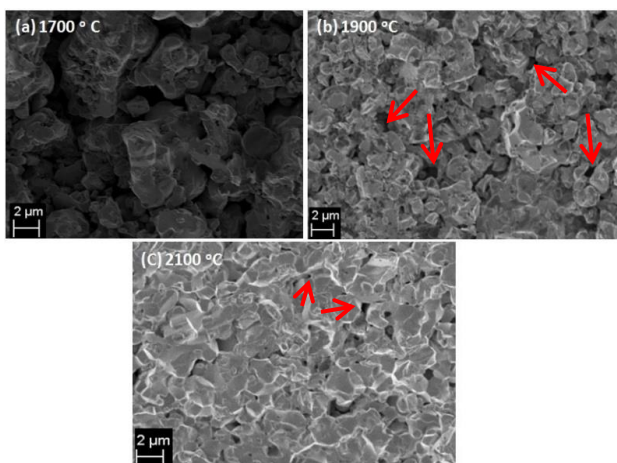


**Fig. 4. SEM micrographs of (a) ZrC ceramic sintered at 1700 °C, (b) at 1900 °C and (c) at 2100 °C by SPS.**

## REFERENCES

1. H.O. Pierson, *Handbook of Refractory Carbides and Nitrides: Properties, Characteristics, and Applications* (Westwood, NJ, (1996).
2. K. Upadhyaya, J.-M. Yang, W.P. Hoffman, *Materials for ultrahigh temperature structural applications*, *Am. Ceram. Soc. Bull.* 76 (1997) 51–56.
3. R. Savino, M.D.S. Fumo, L. Silvestroni, D. Sciti, *Arc-jet testing on HfB<sub>2</sub> and HfC-based ultra-high temperature ceramic materials*, *J. Eur. Ceram. Soc.* 28 (2008) 1899–1907.
4. H.J. Ryu, Y.W. Lee, S. Il Cha, S.H. Hong, *Sintering behaviour and microstructures of carbides and nitrides for the inert matrix fuel by spark plasma sintering*, *J. Nucl. Mater.* 352 (2006) 341–348.
5. E. Min-Haga, W.D. Scott, *Sintering and mechanical properties of ZrC-ZrO<sub>2</sub> composites*, *J. Mater. Sci.* 23 (1988) 2865–2870.
6. O.O. Ozturk, G. Goller, *Spark plasma sintering and characterization of ZrC-TiB<sub>2</sub> composites*, *Ceram. Int.* 43 (2017) 8475–8481.
7. S.-K. Sun, G.-J. Zhang, W.-W. Wu, J.-X. Liu, T. Suzuki, Y. Sakka, *Reactive spark plasma sintering of ZrC and HfC ceramics with fine microstructures*, *Scr. Mater.* 69 (2013) 139–142.
8. X. Wei, C. Back, O. Izhvanov, C.D. Haines, E.A. Olevsky, *Zirconium carbide produced by spark plasma sintering and hot pressing: Densification kinetics, grain growth, and thermal properties*, *Materials* (Basel). 9 (2016) 577.
9. T. Suzuki, H. Matsumoto, N. Nomura, S. Hanada, *Microstructures and fracture toughness of directionally solidified Mo--ZrC eutectic composites*, *Sci. Technol. Adv. Mater.* 3 (2002) 137–143.
10. J.Y. Ko, S.-Y. Park, D.Y. Yoon, S.-J.L. Kang, *Migration of Intergranular Liquid Films and Formation of Core-Shell Grains in Sintered TiC--Ni Bonded to WC--Ni*, *J. Am. Ceram. Soc.* 87 (2004) 2262–2267.
11. W.G. Fahrenholtz, E.J. Wuchina, W.E. Lee, Y. Zhou, *Ultra-high temperature ceramics: materials for extreme environment applications*, *John Wiley & Sons*, 2014.
12. Z.A. Munir, U. Anselmi-Tamburini, M. Ohyanagi, *The effect of electric field and pressure on the synthesis and consolidation of materials: a review of the spark plasma sintering method*, *J. Mater. Sci.* 41 (2006) 763–777.
13. D.S. Perera, M. Tokita, S. Moricca, *Comparative study of fabrication of Si<sub>3</sub>N<sub>4</sub>/SiC composites by spark plasma sintering and hot isostatic pressing*, *J. Eur. Ceram. Soc.* 18 (1998) 401–404.
14. L. Kljajević, S. Nenadović, M. Nenadović, D. Gautam, T. Volkov-Husović, A. Devečerski, B. Matović, *Spark plasma sintering of ZrC--SiC ceramics with LiYO<sub>2</sub> additive*, *Ceram. Int.* 39 (2013) 5467–5476.
15. A. Zavaliangos, J. Zhang, M. Krammer, and J. R. Groza, *Temperature evolution during field activated sintering*, *Mater. Science Eng. A*, vol. 379, pp. 218–228, 2004.
16. G.D. Zhan, A.K. Mukherjee, *Carbon Nanotube Reinforced Alumina-Based Ceramics with Novel Mechanical, Electrical, and Thermal Properties*, *Appl. Ceram. Technol.* 71 (2004) 161–171.
17. R. Delhez, T.H. De Keijser, E.J. Mittemeijer, *Determination of crystallite size and lattice distortions through X-ray diffraction line profile analysis*, *Fresenius' Zeitschrift für Anal. Chemie.* 312 (1982) 1–16.
18. T.B.M. C.S. Barrett, *Structure of Metals*, Pergamon Press. Oxford, UK. (1980).
19. D. Sciti, S. Guicciardi, M. Nygren, *Spark plasma sintering and mechanical behaviour of ZrC-based composites*, *Scr. Mater.* 59 (2008) 638–641.
20. S. K. Sun, G. J. Zhang, W. W. Wu, J. X. Liu, T. Suzuki, and Y. Sakka, *Reactive spark plasma sintering of ZrC and HfC ceramics with fine microstructures*, *Scr. Mater.*, vol. 69 (2013) 139–142.

21. W. K. Burton, N. Cabrera and F. C. Frank, *The growth of crystals and the equilibrium structure of their surfaces*, *Phil. Trans. Roy. Soc. A* 243 (1951) 299- 358.
22. J. P. Hirth and G. M. Pound, *Coefficients of evaporation and condensation*, *J. Phys. Chem.* 64 (1960) 619–626.
23. D. Sciti, M. Nygren, *Spark plasma sintering of ultra refractory compounds*, *J. Mater. Sci.* 43 (2008) 6414–6421.
24. C.V. Thompson, *Structure evolution during processing of polycrystalline films*, *Annu. Rev. Mater. Sci.* 30 (2000) 159–190.
25. X. Wei, C. Back, O. Izhvanov, O.L. Khasanov, C.D. Haines, E.A. Olevsky, *Spark plasma sintering of commercial zirconium carbide powders: Densification behavior and mechanical properties*, *Materials (Basel)*. 8 (2015) 6043–6061.

**Important:** Articles are published under the responsibility of authors, in particular concerning the respect of copyrights. Readers are aware that the contents of published articles may involve hazardous experiments if reproduced; the reproduction of experimental procedures described in articles is under the responsibility of readers and their own analysis of potential danger.

### **Reprint freely distributable – Open access article**

**Materials and Devices is an Open Access journal** which publishes original, and **peer-reviewed** papers accessible only via internet, freely for all. Your published article can be freely downloaded, and self archiving of your paper is allowed and encouraged!

We apply « **the principles of transparency and best practice in scholarly publishing** » as defined by the Committee on Publication Ethics (COPE), the Directory of Open Access Journals (DOAJ), and the Open Access Scholarly Publishers Organization (OASPA). The journal has thus been worked out in such a way as complying with the requirements issued by OASPA and DOAJ in order to apply to these organizations soon.

**Copyright** on any article in Materials and Devices is retained by the author(s) under the Creative Commons (Attribution-NonCommercial-NoDerivatives 4.0 International (CC BY-NC-ND 4.0)), which is favourable to authors.



**Aims and Scope of the journal** : the topics covered by the journal are wide, Materials and Devices aims at publishing papers on all aspects related to materials (including experimental techniques and methods), and devices in a wide sense provided they integrate specific materials. Works in relation with sustainable development are welcome. The journal publishes several types of papers : A: regular papers, L : short papers, R : review papers, T : technical papers, Ur : Unexpected and « negative » results, Conf: conference papers.

(see details in the site of the journal: <http://materialsanddevices.co-ac.com>)

We want to maintain Materials and Devices Open Access and free of charge thanks to volunteerism, the journal is managed by scientists for science! You are welcome if you desire to join the team!

**Advertising in our pages helps us!** Companies selling scientific equipments and technologies are particularly relevant for ads in several places to inform about their products (in article pages as below, journal site, published volumes pages, ...). Corporate sponsorship is also welcome!

**[Feel free to contact us! contact@co-ac.com](mailto:contact@co-ac.com)**